



# Synthesis, characterization and catalytic performance of LSCF perovskite for VOC combustion

Mirosław Zawadzki<sup>a,\*</sup>, Janusz Trawczyński<sup>b</sup>

<sup>a</sup> Institute of Low Temperature and Structure Research, Polish Academy of Sciences, P.O. Box 1410, 50-950 Wrocław 2, Poland

<sup>b</sup> Wrocław University of Technology, Gdańska St. 7/9, 50-344 Wrocław, Poland

## ARTICLE INFO

### Article history:

Received 14 September 2010

Received in revised form 18 October 2010

Accepted 19 October 2010

Available online 20 November 2010

### Keywords:

Perovskites

$\text{La}_{1-x}\text{Sr}_x\text{Co}_{1-y}\text{Fe}_y\text{O}_3$

Ethanol combustion

$\text{C}_3$ – $\text{C}_4$  alkanes total oxidation

## ABSTRACT

Perovskite-type  $\text{La}_{0.6}\text{Sr}_{0.4}\text{Co}_{0.2}\text{Fe}_{0.8}\text{O}_3$  (LSCF) mixed oxides were successfully prepared by combustion and reactive grinding method, characterized by XRD, ICP, XPS, TEM, SEM, TPR- $\text{H}_2$ ,  $\text{N}_2$  adsorption–desorption and acid–base measurements and their catalytic activities for combustion of  $\text{C}_3$ – $\text{C}_4$  alkanes and ethanol were determined. LSCF materials show good catalytic performances: 100% conversion of  $\text{C}_3$ – $\text{C}_4$  and ethanol can be reached below 400 and 260 °C, respectively, and activity was stable with extended time on stream and for repeated temperature cycles as well. LSCF materials seem then to be promising alternative to noble metal based catalysts for VOC oxidation.

© 2010 Elsevier B.V. All rights reserved.

## 1. Introduction

During the last decades, there has been increasing concern for the environment protection due to the emission of different pollutants to the atmosphere. The emission of VOCs has received particular attention as they have been established to cause many serious environmental problems. Some VOCs are directly harmful (carcinogenic, nervously paralyzed, uncomfortable, etc.) and others have involvement in the formation of photochemical smog, acidic rain, greenhouse effect or depletion of stratospheric ozone layer. Catalytic combustion processes is recognized as convenient way for VOCs emission prevention [1].

Perovskite-type oxides are widely studied for the application in oxygen separation [2] and solid oxide fuel cells [3]. Besides, they display prominent catalytic activities in many fields including total oxidation of VOCs [4], causing that they are postulated as potential substitutes of noble metals, very active but more expensive and less thermal stable. Some perovskites have recently been shown as promising materials for this purpose, among others  $\text{LaCoO}_3$  partially substituted with Sr or Fe on the A and B sites, respectively.  $\text{La}_{1-x}\text{Sr}_x\text{CoO}_3$  was found to show enhanced activity for propanol/cyclohexane total oxidation [5] while  $\text{LaCo}_{1-x}\text{Fe}_x\text{O}_3$  for *n*-hexane combustion [6], as compared to the activity of non-substituted  $\text{LaCoO}_3$  for these reactions. So far, there are only a few literature data concerning the catalytic properties of perovskite-

like mixed oxide  $\text{La}_{1-x}\text{Sr}_x\text{Co}_{1-y}\text{Fe}_y\text{O}_{3-\delta}$  (LSCF) – it was found as a good catalyst for combustion of methane [7] and toluene [8] or methanol decomposition [9]. For these reasons, we prepared LSCF mixed oxides and characterized them as catalyst for pollution abatement. In this study, catalytic behaviour of LSCF was evaluated in combustion of  $\text{C}_3$ – $\text{C}_4$  alkanes and ethanol. Efficient and no expensive catalyst for the complete destroying of such VOCs at low concentrations is essential because mixture of propane and butanes (as LPG), and (bio)ethanol are increasingly used as a substitute for gasoline and diesel in transport vehicles. Furthermore, short chain alkanes, recognized as the most difficult to destroy, are emitted from a range of stationary sources and their treatment is a priority.

## 2. Experimental

Materials with formal composition  $\text{La}_{0.6}\text{Sr}_{0.4}\text{Co}_{0.2}\text{Fe}_{0.8}\text{O}_3$  were prepared via glycine-nitrate process (C sample) and wet ball-milling method (G sample). The first one is self-sustaining combustion synthesis technique which can produce fine and homogeneous mixed metal oxides powders. Glycine serves here a dual role: it complexes the metal cations in the precursor solution and next, upon ignition, the oxidized (by the nitrates) glycine becomes a fuel for the combustion reaction. Further thermal treatment at temperatures above 800 °C is needed. The second one, reactive grinding method, is performed at essentially room temperature and may directly yield materials with desired structure but it requires prolonged time of milling with high energy consumption. For short milling times, mechanosynthesis allows the reactivity of the precursors to be increased but must be followed by additional heat

\* Corresponding author.

E-mail address: [m.zawadzki@int.pan.wroc.pl](mailto:m.zawadzki@int.pan.wroc.pl) (M. Zawadzki).

treatment. Both methods have advantages over classical routes of complex oxides preparation (e.g. ceramic) leading to the nanocrystalline materials with interesting surface properties. In the case of C preparation, aqueous solution of metal nitrates and glycine was placed in the oven where after water evaporation spontaneous combustion occurred (heating temperature up to 350 °C). G sample was prepared by milling of stoichiometric mixture of corresponding oxides ( $\text{La}_2\text{O}_3$ ,  $\text{Fe}_2\text{O}_3$ ,  $\text{Co}_2\text{O}_3$ ) and  $\text{SrCO}_3$  in ethanol for 2 h using attritor ( $d = 135$  mm,  $h = 180$  mm, 4.6 kg of stainless steel balls ( $d = 3$  mm),  $\text{rpm} = 280 \text{ min}^{-1}$ ). Finally, both samples were heated at 850 °C for 6 h then were lightly milled to obtain a fine powder, which was compressed into tablets, then crushed and sieved into the pieces of 0.6–1.2 mm.

The crystal structure was determined by powder X-ray diffraction (XRD). The crystallite size was calculated based on the Scherrer equation. The elemental analysis was carried out by using the inductively coupled plasma (ICP) method. The morphology was observed by a transmission electron microscopy (TEM) and a scanning electron microscopy (SEM). The specific surface area was determined by the BET method from nitrogen adsorption data obtained in a volumetric system. Surface composition was characterized by X-ray photoelectron spectroscopy (XPS). Temperature programmed reduction (TPR- $\text{H}_2$ ) experiments were performed in a flow apparatus using a mixture of  $\text{H}_2$  (6.5 vol.%) in argon at temperature range 20–950 °C. Acid-basic properties were determined by analysis of results of cyclohexanol (CHOL) decomposition on the

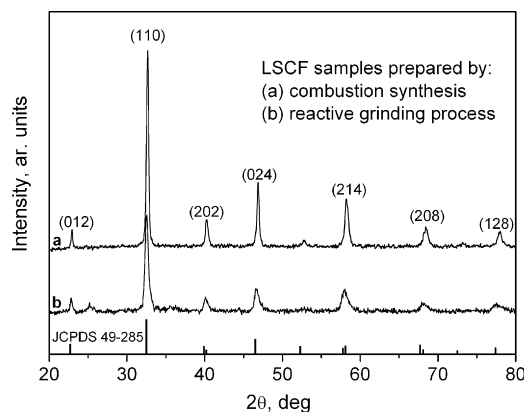


**Fig. 1.** XRD patterns of LSCF materials: C sample (a), G sample (b); for phase identification purpose, standard diffraction pattern (JCPDS File No. 49-285) is also shown.

studied materials. Tests were carried out in a continuous-flow fixed bed quartz reactor (8 mm i.d.) placed in a tube furnace. The catalyst (0.5 g) was held on quartz wool, total gas flow 20 dm<sup>3</sup>/h (dry  $\text{N}_2$  99.999%) saturated with CHOL (2.6 mmol/h) was used, and reaction temperature was fixed at 300 °C. Products of the reaction were analysed using gas chromatograph equipped with FID detector. Total conversion of CHOL and both yield and selectivity to cyclo-

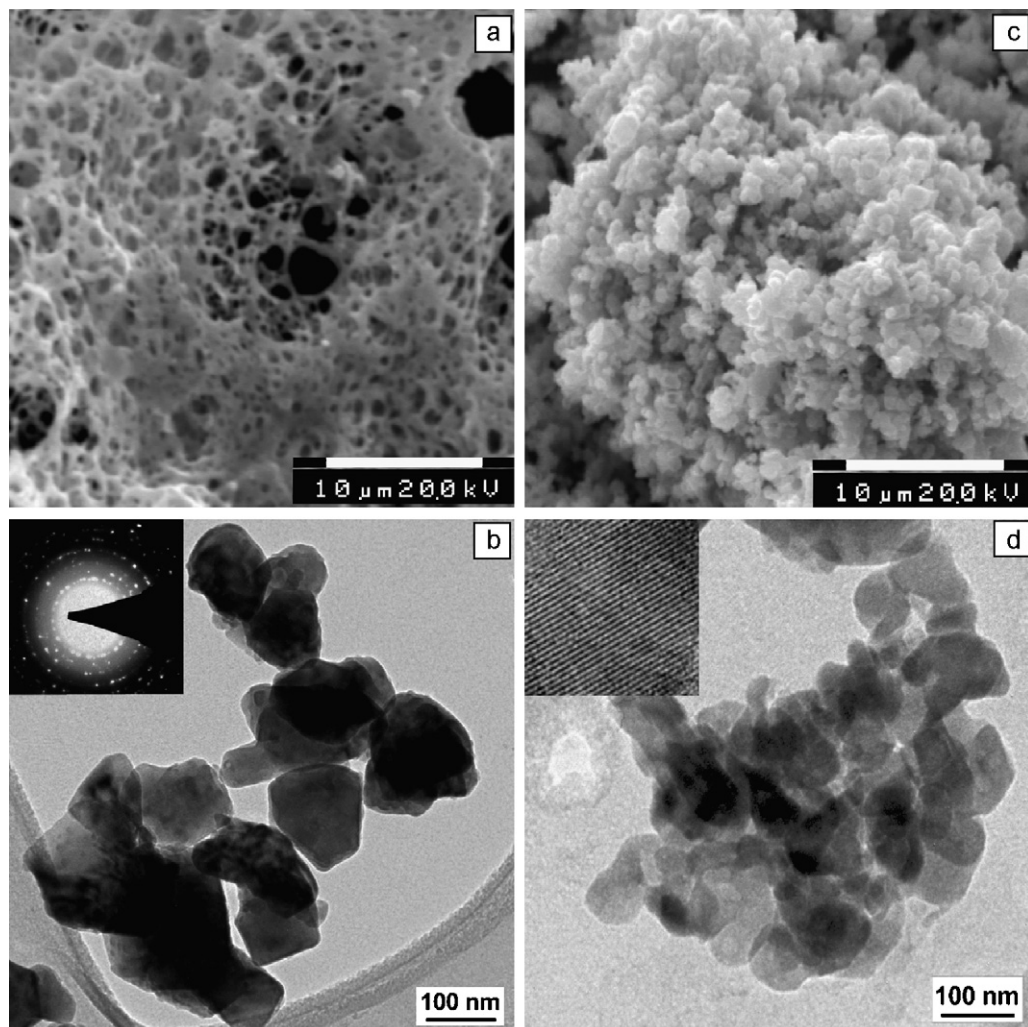


**Fig. 2.** SEM and TEM images of LSCF materials: C (a and b) and G (c and d) sample, with SAED pattern (inset in b) and HRTEM image (inset in d).

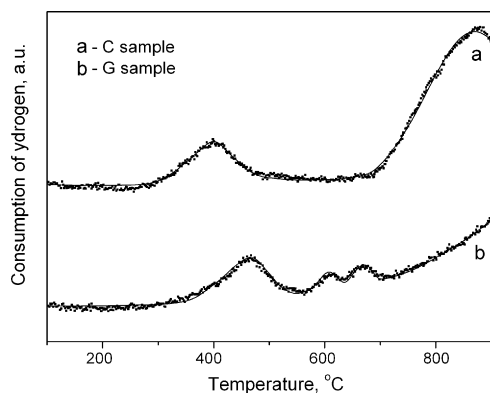


Fig. 3. TPR-H<sub>2</sub> profiles of LSCF materials.

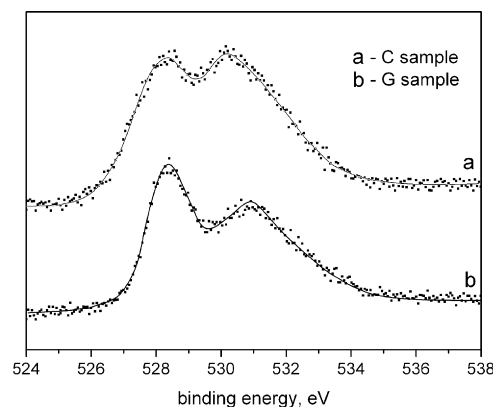


Fig. 4. O 1s XPS spectra of LSCF materials.

hexene (CHEN) and cyclohexanone (CHON) were determined. The total acidity and the acid strength distribution were evaluated by the temperature-programmed desorption of ammonia (TPD-NH<sub>3</sub>) method. The sample (2 g) was heated to 750 °C in argon flow for 1 h then cooled to 180 °C. Adsorption of pure ammonia was performed for 0.5 h followed by a purge with argon at 180 °C for 1 h to remove physically adsorbed NH<sub>3</sub>. Finally, TPD-NH<sub>3</sub> measurements were started in argon with a heating rate 10°/min. Amounts of desorbed ammonia were analysed using a gas chromatograph with a TCD detector. The catalytic activity measurements were carried out in a fixed-bed flow reactor made of quartz tubing of 10 mm i.d., placed in a programmable furnace, by passing a gaseous mixture of reactants and air over 1 g catalyst (bed height ~1 cm). The reaction feed consisted of 2000 vppm VOC in air, and total flow rate was 15 l/h to give GHSV of 21.000 h<sup>-1</sup>. Analysis was performed by an on-line gas chromatograph with a FID detector.

### 3. Results and discussion

XRD patterns (Fig. 1) confirmed the formation of the perovskite structure with the expected rhombohedral phase symmetry: C shows the presence of pure perovskite phase while a trace of SrCO<sub>3</sub> (at  $2\theta = 25.2$  and  $25.8^\circ$ ) appeared in G. The presence of sharp and strong diffraction peaks suggests the high crystallinity of obtained materials. Average crystallite size for C and G is 26 and 16 nm, respectively. Composition of these materials is very close to the desired one, as was revealed by ICP analysis – La<sub>0.600</sub>Sr<sub>0.398</sub>Co<sub>0.199</sub>Fe<sub>0.802</sub>O<sub>3</sub> for C and La<sub>0.600</sub>Sr<sub>0.396</sub>Co<sub>0.197</sub>Fe<sub>0.806</sub>O<sub>3</sub> for G. Both samples show relatively low specific surface area ( $S_{\text{BET}}$ ), i.e. 4.4 and 3.4 m<sup>2</sup>/g, respectively for C and G. SEM images (Fig. 2a and c) reveal different morphology of studied materials: typical macroporous network (C) or characteristic agglomerates with irregular shape (G). According to TEM images (Fig. 2b and d), one can observe that most of particles are quasi-spherical, and grain sizes are 50–100 nm for C, while for G amount to 20–30 nm. HRTEM studies (inset in Fig. 2d) showed that particles are well-crystallized exhibiting lattice fringes of distance 0.27 nm that corresponds to the (1 1 0) lattice plane of LSCF structure. The crystallography of the samples is also proven by SAED pattern (inset in Fig. 2b): diffraction rings/spots match the XRD peaks very well. Two main signals of hydrogen consumption can be distinguished on TPR-H<sub>2</sub> profiles (Fig. 3) of both materials however they differ in temperatures of peak maximum. The first peak has maximum at 400 and 470 °C while the second at ~900 and above 900 °C, respectively for C and G. Additionally, high temperature TPR-H<sub>2</sub> signal of G is composed of two smaller peaks with maximum at 610 and 670 °C. One can suppose that on the surface of G any impurities, e.g. unreacted raw materials are present. Results of CHOL decomposition and TPD-NH<sub>3</sub> measurements revealed that both samples

posses low total acidity (0.014 and 0.010 mmol NH<sub>3</sub>/m<sup>2</sup>, respectively for C and G) but G presents relatively higher share of basic sites (CHON/CHEN selectivity ratio amounts to 4.3 for C and 5.3 for G) and lower share of acidic ones ( $T_{\text{NH}_3 \text{ desorption}} < 450^\circ\text{C}$ ) than C. Data from XPS analysis suggest that surface composition is quite far from stoichiometric calculations and is different for C and G: surface of C is relatively enriched in cobalt, iron is less exposed, while surface layers of G exhibit higher content of strontium and iron, but lanthanum is poorly exposed. Fig. 4 shows XPS spectra for O 1s of both materials, which suggest that two different types of oxygen species on the LSCF surface are present: lattice oxygen ( $\beta$ -oxygen, metal bonded oxygen O<sup>2-</sup>) at lower BE values and chemisorbed oxygen ( $\alpha$ -oxygen, e.g. O<sup>-</sup>) at higher BE values. Peaks assigned to lattice oxygen has maximum at  $528.4 \pm 0.1$  eV independently on the method of synthesis. However in the case of chemisorbed oxygen species position of BE maximum is different and for C is located at  $530.2 \pm 0.1$  eV while for G it is at  $531.0 \pm 0.1$  eV. It means that the oxygen species ( $\alpha$ -oxygen) present on the surface of C are different than those ones on the surface of G. It is known that on the surface of mixed oxides with perovskite-like structure, different species of adsorbed oxygen are formed. These species are gradually enriched with electrons (O<sub>2</sub><sup>-</sup>, O<sub>2</sub><sup>2-</sup>) and finally the typical surface lattice oxygen is formed [10]. Because partially reduced surface oxygen species are strongly electrophilic (that means reactive in oxidation reactions). One can expect that materials exhibiting higher concentration of such species will be more active in oxidation reactions.

The results of C<sub>3</sub>–C<sub>4</sub> alkanes and ethanol combustion are collected in Fig. 5. One may see that both LSCF materials show good catalytic performances in studied reactions, but for C the reaction light-off temperature, the characteristic temperature at which 50% conversion is reached and full conversion temperature of the reactants are slightly lower. Different catalytic activity of C and G should be attributed to the presence of different oxygen species on their surface. Indeed, the main difference between both samples is the relative ease with which oxygen species can be released from the surface of studied materials during TPR-H<sub>2</sub> experiments. It can be assumed that catalytic activity of LSCF materials in studied reactions is controlled by the nonstoichiometric character of their surface and the presence of various oxygen species on their surfaces. As it was confirmed by results of XPS and TPR-H<sub>2</sub> characterization, on the surface of studied materials oxygen species differing in electron density (degree of reduction) are present. These ones present on C are more electrophilic (higher BE of O1s for C) and are reduced at lower temperature (first reduction peak of C has maximum appearing at lower temperature than corresponding one of G). It is known that electrophilic oxygen species are very active in oxidation reactions. Many reports confirm that loosely bonded oxygen species present on surface exhibit high activity for

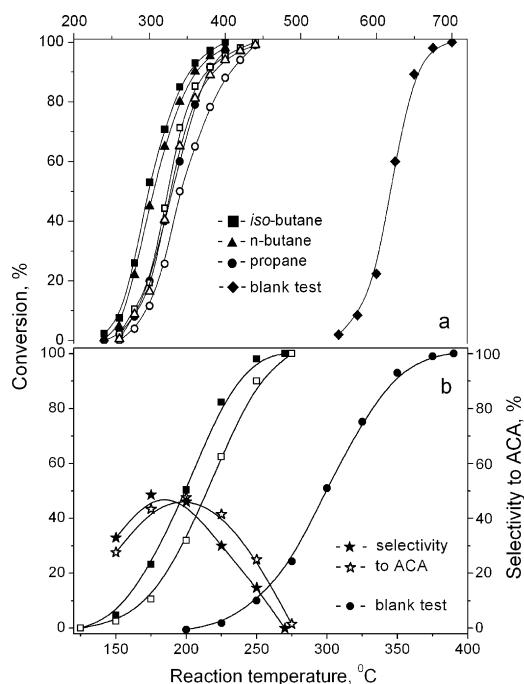


**Fig. 5.** Conversion of C<sub>3</sub>–C<sub>4</sub> (a) and ethanol (b), and selectivity to acetaldehyde (ACA) over C (solid symbols) and G (open symbols) samples.

total oxidation [11]. The activity of LSCF materials with time on stream (up to 10 h) for both reactions was also investigated: the conversion was found to be stable and no deactivation was evident. No significant changes in the light-off curves for repeated temperature cycles (up to 6 times) were also found.

#### 4. Conclusions

The presented results show that glycine-nitrate and ball-milling processes are powerful in synthesis of perovskite-type materials with the formal composition  $\text{La}_{0.6}\text{Sr}_{0.4}\text{Co}_{0.2}\text{Fe}_{0.8}\text{O}_3$  as active catalyst with promising stability for total oxidation of C<sub>3</sub>–C<sub>4</sub> alkanes and ethanol. Combustion synthesis was found to be more useful and convenient in preparing such complex oxides leading to their better catalytic performances. High catalytic activity of studied materials can be related with generation of readily accessible active sites (electrophilic surface oxygen species) due to the specific composition of surface layer. Though LSCF materials show very promising performances in oxidation reactions providing an alternative to noble metal based catalysts, further work will be crucial to determine if such prepared catalysts are promising ones if real gases (usually complex mixtures) need to be treated.

#### References

- [1] W.B. Li, J.X. Wang, H. Gong, Catal. Today 148 (2009) 81–87.
- [2] L. Ge, R. Ran, W. Zhou, Z. Shao, S. Liu, W. Jin, N. Xu, J. Membr. Sci. 329 (2009) 219–227.
- [3] J. Sacanell, M.G. Bellino, D.G. Lamas, A.G. Leyva, Physica B 398 (2007) 341–343.
- [4] R. Spinicci, M. Faticanti, P. Marini, S. de Rossi, P. Porta, J. Mol. Catal. A 197 (2003) 147–155.
- [5] H. Huang, Y. Liu, W. Tang, Y. Chen, Catal. Commun. 9 (2008) 55–59.
- [6] V. Szabo, M. Bassir, A. Van Neste, S. Kaliaguine, Appl. Catal. B 37 (2002) 175–180.
- [7] M. Alifanti, J. Kirchnerova, B. Delmon, D. Klvana, Appl. Catal. A 262 (2004) 167–176.
- [8] N. Li, A. Boréave, J.-P. Deloume, F. Gaillard, Solid State Ionics 179 (2008) 396–400.
- [9] A. Galenda, M.M. Natile, A. Glisenti, J. Mol. Catal. A 282 (2008) 52–61.
- [10] N.A. Merino, B.P. Barbero, P. Eloy, L.E. Cadús, Appl. Surf. Sci. 253 (2006) 1489–1493.
- [11] I.S. Yakovleva, L.A. Isupova, V.A. Rogov, Kinet. Catal. 50 (2009) 275–283.